Synthesis and Structural Study of [5.5](2,6)Pyridinophanes and -cyclophanes Containing Silylene Units†

Bernadette Rezzonico and Micheline Grignon-Dubois*

Laboratoire de Chimie Organique et Organométallique, CNRS UMR 5802, Université Bordeaux I, 351, Cours de la Libération, F-33405 Talence-Cedex, France

Michel Laguerre

CRPP, UPR 8641, Avenue du Docteur Albert Schweitzer, F-33600 Pessac, France

Jean-Michel Léger

Laboratoire de Chimie Analytique, UFR des Sciences Pharmaceutiques, Université Bordeaux 2, 3, place de la Victoire, F-33076 Bordeaux-Cedex, France

Received June 6, 1997

Four [5.5](2,6)pyridinophanes and -cyclophanes containing silylene units (**2a**,**b**, **3a**,**b**) have been prepared by reacting dichlorosilanes with pyridine- or benzenedimethanol. X-ray structures of compounds **2a**, **2b**, and **3a** have been determined. The diphenylsilylene pyridinophane **2b** and dimethylsilylene cyclophane **3a** were found to adopt an *anti* conformation in the solid state. In contrast, the dimethylsilylene pyridinophane **2a** exhibits a *syn* arrangement. The conformational preference of these cyclophanes without the influence of the packing energy was analyzed by molecular mechanics calculations. The results show that all the derivatives preferentially adopt a *syn* conformation, whereas the *anti* geometry found in the solid state for **2b** and **3a** does not play a significant role in the conformational equilibrium at room temperature.

Introduction

Due to their unusual geometry and potential as complexants, mobile macrocycles have gained great importance.[1] In the case of [*m*.*m*]metacyclophanes, the conformational equilibrium has been reported to be dependent on the bridging chain lengths *m*. When *m* = 2, it is completely shifted toward an *anti* form as long as there is at least one internal aryl hydrogen,[2] but *syn* forms were also reported with or without internal substituents.[3] In contrast, the *syn* isomer seems to be generally favored when *m* = 3.[2d,3b,c,4] However, *anti* structures were demonstrated for [3.3]metacyclophane-2,11-dione derivatives.[5] Anticlinal and edge-to-face conformations have been respectively established for tetramethyl-[6a,b] and dithia[4.4]metacyclophanes.[6c] In contrast to this abundant literature, only a few articles have been devoted to metacyclophanes having longer bridging. Bradshaw *et al.* have reported an *anti* structure for a tetramethyl[6.6](2,6)pyridinophane,[7] whereas a hexathia[9.9]metacyclophane was shown to be curled in on itself.[8] As part of our study of the synthesis and conformation for the [5.5](2,6)pyridinophane series, we planned to incorporate a silicon unit in the bridge. At the beginning of this work, some examples of silicon-bridged macrocycles had been described,[9] but no sila-[5.5]pyridinophanes, despite their potential interest. Indeed, silicon presents many advantages for the design

* To whom correspondence should be addressed. Tel: 33 56846286. Fax: 33 56846646. E-mail: m.grignon@lcoo.u-bordeaux.fr.

† Dedicated to Daniel Farge, who initiated this work.

(1) See, for example: (a) Majestic, V. K.; Newkome, G. R. *Top. Curr. Chem.* **1982**, *106*, 79. Diederich, F. *Cyclophanes;* Stoddart, J. F., Ed.; Monographs in Supramolecular Chemistry; The Royal Society of Chemistry: Cambridge, U.K., 1991; Vol. 2. (b) Vögtle, F. *Cyclophane Chemistry*; Wiley: New York, 1993. (c) Huszthy, P.; Oue, M.; Bradshaw, J. S.; Zhu, C. Y.; Wang, T.; Dalley, N. K.; Curtis, J. C.; Izatt, R. M. *J. Org. Chem.* **1992,** *57*, 5383 and references therein.

(2) (a) Misumi, S.; Otsubo, T. *Acc. Chem. Res.* **1978**, *11*, 251. (b) Vögtle, F.; Neumann, P. *Angew. Chem., Int. Ed. Engl.* **1993**, *32*, 601. (c) Güther, R.; Nieger, M.; Vögtle, F. *Angew. Chem., Int. Ed. Engl.* **1972**, *11*, 73. (d) Lai, Y.-H.; Mok, K. F.; Ting, Y. *J. Org. Chem.* **1994**, *59*, 7345.

(3) (a) Tashiro, M.; Fujimoto, H.; Tsuge, A.; Mataka, S.; Kobayashi, H. *J. Org. Chem.* **1989,** *54*, 2012. (b) Mitchell, R. H.; Vinod, T. K.; Bushnell, G. W. *J. Am. Chem. Soc.* **1990**, *112*, 3487. (c) Sako, K.; Tatemitsu, H.; Onaka, S.; Takemura, H.; Osada, S.; Wen, G.; Rudzinski, J. M.; Shinmyozu, T. *Liebigs Ann. Chem.* **1996**, 1645.

(4) (a) Fukazawa, Y.; Takeda, Y.; Usui, S.; Kodama, M. *J. Am. Chem. Soc.* **1988**, *110*, 7842. (b) Mitchell, R. H.; Vinod, T. K.; Bodwell, J.; Bushnell, G. W. *J. Org. Chem.* **1989,** *54*, 5871.

(5) (a) Fukazawa, Y.; Hayashibara, T.; Yang, Y.; Usui, S. *Tetrahedron Lett.* **1995,** *36*, 3349. (b) Breitenbach, J.; Hoss, R.; Nieger, M.; Rissanen, K.; Vögtle, F. *Chem. Ber.* **1992**, *125*, 255.

(6) (a) Fukazawa, Y.; Ogata, K.; Usui, S. *J. Am. Chem. Soc.* **1988**, *110*, 8692. (b) Fukazawa, Y.; Usui, S.; Tanimoto, K.; Hirai, Y. *J. Am. Chem. Soc.* **1994**, *116*, 8169. (c) Schladetzky, K. D.; Haque, T. S.; Gellman, S. H. *J. Org. Chem.* **1995**, *60*, 4108.

(7) Bradshaw, J. S.; Huszthy, P.; McDaniel, C. W.; Zhu, C. Y.; Dalley, N. K.; Izatt, R. M. *J. Org. Chem.* **1990**, *55*, 3129.

(8) de Groot, B.; Loeb, S. J.; Shimizu, G. K. H. *Inorg. Chem.* **1994**, *33*, 2663.

(9) See, for example: (a) Gleiter, R.; Shafer, W. *J. Am. Chem. Soc.* **1988**, *110*, 4117. (b) Launay, N.; Denat, F.; Caminade, A.-M.; Majoral, J.-P.; Dubac, J. *Bull. Soc. Chim. Fr.* **1994**, *131*, 758. (c) Marcus, L.; Klingebiel, U.; Noltemeyer, M. *Z. Naturforsch.* **1994**, *50B*, 687. (d) Kaes, C.; Hosseini, M. W.; Ruppert, R.; De Cian, A.; Fischer, J.-P. *Tetrahedron Lett.* **1994**, *35*, 7233. (e) König, B.; Rödel, M.; Bubenitschek, P.; Jones, P. G. *Angew. Chem., Int. Ed. Engl.* **1995**, *34*, 661 and references therein.

S0276-7333(97)00475-5 CCC: $15.00
Publication on Web 05/21/1998

Chart 1

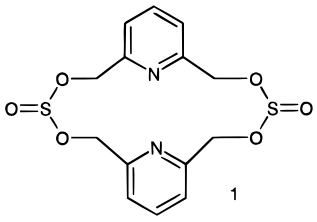

1

of new macrocycles. In particular, it can serve as an additional coordination site as well as a means of increasing the solubility and the flexibility. We have recently described the preparation of 1,3,11,13-tetraoxo-2,12-dithia[5.5](2,6)pyridinophane-2,12-dioxide (**1**) by reacting thionyl chloride with 2,6-pyridinedimethanol.[10] This prompted us to extend this process to the silyl analogues, simply replacing thionyl chloride with dichlorosilanes. In the present paper, we report the synthesis and structural study of 1,3,11,13-tetraoxo-2,12-(dialkylsilylene)[5.5](2,6)pyridinophanes (**2a, 3a**) and 1,3,-11,13-tetraoxo-2,12-(dialkylsilylene)[5.5]metacyclophanes (**2b**, **3b**) (Chart 1).

Results and Discussion

The cyclic dimers **2** and **3** were prepared by reacting dichlorosilane and 2,6-pyridine- or benzenedimethanol in the presence of Et_3N, as shown in Scheme 1. The 1/1/2 molar ratio was found to be the optimum. The reactions were conducted at reflux or under sonochemical activation (Table 1). The ^1H NMR spectrum of the reaction mixture obtained after removal of triethylamine hydrochloride showed that the diol was completely consumed. In each case, we observed the formation of two main silylated products, which have very similar NMR spectra with the same coupling constants and very similar chemical shifts (see Experimental Section). These mixtures were then taken up in ether, leaving white solids, which were identified as the 2/2 cyclization products **2a**,**b** and **3a**,**b**. They are readily soluble in chloroform or dichloromethane, with the exception of **3b**, which is almost insoluble in all the usual solvents. Evaporation of the ethereal solutions led to the oligomeric products **2c,d** and **3c**,**d**. No trace of the 1/1 cyclization products was found. Molecular modeling of the monomers suggests that this may be due to the severe strain imposed by an excessively short bridge, which forces the aromatic ring to distort into a shallow boat form.

The influence of the experimental conditions on the reaction outcome was carefully studied in the case of the condensation of dimethyldichlorosilane with pyridinedimethanol (Table 1). Heating overnight without solvent led to the oligomer **2c** as the only product (80% yield). In dichloromethane at reflux (24 h), **2a** was obtained in 20% yield along with a mixture of oligomers. This yield decreased to 15% under sonochemical activation at room temperature. In contrast, when benzene was used as the solvent, **2a** was isolated in 20% yield after a 24 h reflux and 36% after 3 h of sonication at room temperature. This variation in the yield according to the solvent used in the sonification is in good agreement with the known variation of temperature at which cavitation produced by ultrasonic waves reaches maximun intensity, i.e., 19 °C in the case of benzene and −40 °C in the case of dichloromethane.[11] In the three other cases, the reactions were conducted only in benzene solution at reflux or under sonochemical activation at room temperature. This last procedure led to the best results.

The structures of all these products have been established by NMR, MS, and elemental analysis. While we were completing this work, Holmes *et al.* published the synthesis of **2a**, using a similar procedure.[12] Comparison of their structural data with ours shows the same ^1H characteristics but, surprisingly, an important discrepancy in the ^{29}Si chemical shift although the same solvent was used (−0.74 ppm in this work compared to −8.80 ppm[12]). Also noticeable is the great discrepancy in the melting point (167−168 °C in this work *vs.* 113 °C[12]). As the authors determined the structure of their product by X-ray diffraction, it appears important to obtain an X-ray crystal structure of our sample. The ORTEP drawing (Figure 1) confirms the structure of our product, which adopts a *syn* conformation as described in ref 12. However, comparison of the crystal data reveals polymorphism, which could be due to the solvent used for the crystallization. Indeed, our sample obtained from dichloromethane crystallizes in the orthorhombic crystal system (Table 2), while the sample obtained by Holmes et al. from diethyl ether exhibits a triclinic system.[12] Superimposition of the two X-ray structures (Figure 2) shows that this polymorphism is mainly due to the difference in the conformations of the linkage, the relative positions of the two pyridine rings showing in both cases a *syn* arrangement. The root-mean-square values (RMS) between the two geometries are 0.08 Å if one considers only the pyridine rings and 0.420 Å if one considers all the atoms. These values show that the deviations are very small and cannot explain the 55 °C difference in the melting point. From these results, it appears important to obtain the triclinic crystal system described by Holmes and measure its melting point. This led us to recrystallize **2a** from Et_2O, but unfortunately, the resulting crystals were shown to have the same orthorhombic crystal system as our first sample obtained from dichloromethane. The melting point (168 °C) and ^{29}Si chemical shift (−0.74 ppm) also remained identical with our former measures.

As the work of Holmes et al. was not done under exactly the same conditions as ours, we reproduced their experiment using toluene in place of benzene and heating to 90 °C for 36 h (instead of 80 °C for 18 h). As we previously observed, the ^1H NMR spectrum of the crude mixture obtained after removal of $[Et_3NH]Cl$ showed the absence of 2,6-pyridinedimethanol and the formation of **2a** along with a mixture of oligomers. Attempts to isolate **2a** in this experiment by passing a slow stream of dry nitrogen over the ethereal solution as described by these authors[12] were arduous and led to a mixture of **2a**, oligomers, and 2,6-pyridinedimethanol. In contrast, when the crude mixture was taken up in the minimum amount of ether (see Experimental

(10) Rezzonico, B.; Grignon-Dubois, M. *J. Chem. Res. Synop.* **1994,** 142.

(11) Niemczewski, B. *Ultrasonics* **1980**, 107.

(12) Prakasha, T. K.; Chandrasekaran, A.; Day, R. O.; Holmes, R. R. *Inorg. Chem.* **1996**, *35*, 4342.

Scheme 1

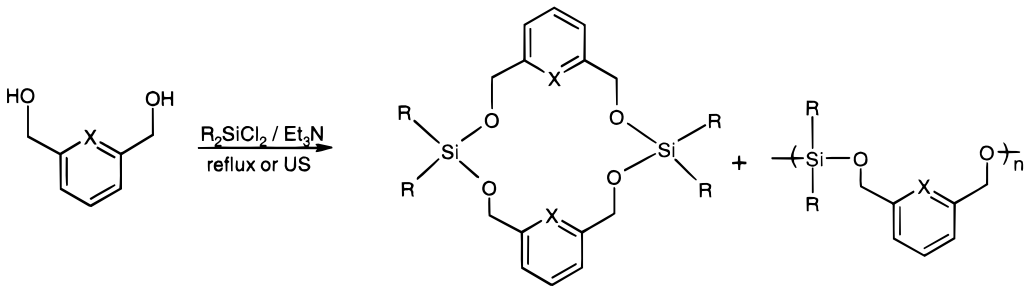

X = N : **2** R = CH_3 **2a** **2c**
R = C_6H_5 **2b** **2d**
X = CH **3** R = CH_3 **3a** **3c**
R = C6H5 **3b** **3d**

Table 1. Reaction of Dichlorosilanes with Pyridine- or Benzenedimethanol

substrate	R in R_2SiCl_2	exptl conditions: solvent	exptl conditions: activation	product yield (%): cyclic dimer	product yield (%): oligomers
2	CH_3	benzene	reflux, 18 h	**2a**: 20	**2c**: 50
		benzene	US, 3 h[a]	**2a**: 36	mixture
		toluene	reflux, 36 h	**2a**: 27	**2c**: 55
		CH_2Cl_2	reflux, 18 h	**2a**: 20	mixture
		CH_2Cl_2	US, 3 h	**2a**: 15	mixture
			80 °C, 18 h		**2c**: 80
2	C_6H_5	benzene	reflux, 18 h	**2b**: 20	mixture
		benzene	US, 3 h	**2b**: 29	mixture
			100 °C, 18 h		**2d**: 91
3	CH_3	benzene	US, 3 h	**3a**: 31	**3c**: 60
		benzene	reflux, 18 h	**3a**: 26	**3c**: 71
3	C_6H_5	benzene	US, 3 h	**3b**: 42	mixture
		benzene	reflux, 18 h	**3b**: 33	**3d**: 60

[a] US = ultrasound.

Section), precipitation of **2a** occurred (21% yield, mp 168 °C), while the oligomers remained in solution. It is worth noting that the oligomers are unstable toward air or oxygen and decompose to polysiloxanes and 2,6-pyridinedimethanol (mp 113 °C).

To confirm that the structure of **2a** remained in solution, ^{29}Si,^{1}H coupling constants were measured using INEPT and SPT experiments (Table 3).[13] Analysis of the spectra confirmed that the ^{29}Si resonance at −0.74 ppm is due to a silicon atom linked to two equivalent methyl groups (six protons coupled with ^{2}J = 7.2 Hz) and two equivalent oxomethylene groups (four protons coupled with ^{3}J = 3.9 Hz). Similar results were obtained with **2b** (Table 3). The dimethylsilylene oligomers show a unique, slightly broadened ^{29}Si signal in the same range, so close to zero in the case of **2c** (−0.02 ppm) that the resonance can be confused with TMS when this reference is used. The ^{1}H NMR spectra are also very similar to those of the cyclic dimer, showing only four rather sharp signals with the same coupling constants and integration. Only the chemical shifts are slightly different, the larger deviation being measured between the dimethylsilylene and the methylene signals: respectively 4.33 ppm for **2a** and 4.60 ppm for **2c**. These data, especially the absence of signals due to termination units for **2c** and **3c**, suggest

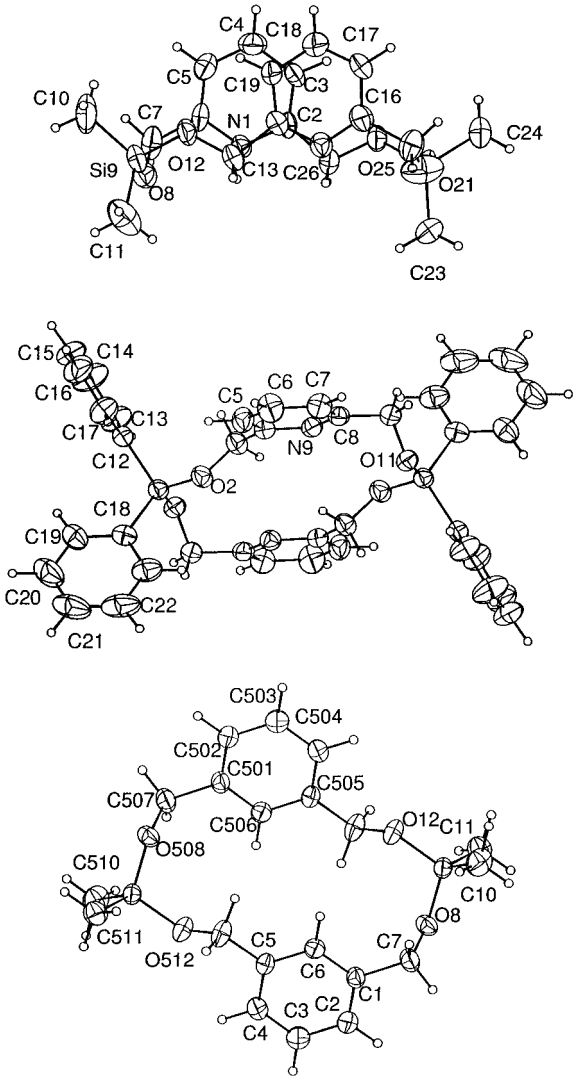

Figure 1. ORTEP drawings of (top) **2a**, (middle) **2b**, and (bottom) **3a**. Atoms are shown with 50% thermal ellipsoids.

that the *n* value is ≥10. In addition, a gel permeation chromatography analysis showed that we have not a unique product, but a mixture. These oligomers are unstable toward air or oxygen and decompose to polysiloxanes and 2,6-pyridinedimethanol (mp 113 °C) or 2,6-benzenedimethanol (mp 57−58 °C). The diphenylsilylene oligomers **2d** and **3d** also decompose on exposure to air, but more slowly.

(13) (a) Blinka, T. A.; Helmer, B. J. *Adv. Organomet. Chem.* **1984**, *23*, 193. (b) Grignon-Dubois, M.; Laguerre, M.; Pétraud, M.; Pianet, I. *Spectrochim. Acta* **1994**, *50A*, 2059 and references therein. (c) Schraml, J. *J. Magn. Reson.* **1984**, *59*, 515.

Table 2. Crystal and Experimental X-ray Data for Compounds 2a,b and 3a

	2a	**2b**	**3a**
empirical formula	$C_{18}H_{26}N_2O_4Si_2$	$C_{38}H_{34}N_2O_4Si_2$	$C_{20}H_{28}O_4Si_2$
fw	390.59	638.9	388.6
cryst syst	orthorhombic	triclinic	monoclinic
space group	$P2_12_12_1$	$P\bar{1}$	$P2_1/c$
a (Å)	6.372(5)	7.478(1)	10.910(1)
b (Å)	13.742(4)	8.951	11.639(2)
c (Å)	23.120(7)	12.995(1)	8.092(1)
α (deg)	90	92.14(1)	
β (deg)	90	91.10(1)	95.46(1)
γ (deg)	90	109.70(1)	
V (Å^3)	2025(2)	818(1)	1022.9(4)
Z	4	1	2
D_C (g cm^{-3})	1.281	1.297	1.262
$F(000)$	832	336	416
λ(Cu Kα) (Å)	1.541 78	1.541 78	1.541 78
scan type	$\omega/2\theta$	$\omega/2\theta$	$\omega/2\theta$
abs coeff (mm^{-1})	1.805	1.313	1.708
temp (K)	296	293	293
θ range for data collection (deg)	$5 < \theta < 65$	$2 < \theta < 65$	$2 < \theta < 65$
no. of data/ restraints/ params	1848/0/236	2378/0/276	581/0/174
final R indices ($I > 3\sigma(I)$)	$R = 0.0858$	$R = 0.041$	$R = 0.052$
	$R_w = 0.2169$	$R_w = 0.053$ $S = 1.28$	$R_w = 0.066$ $S = 2.09$

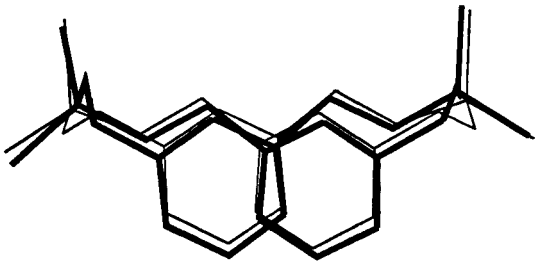

Figure 2. Superimposition of the two X-ray structures of **2a**: (thin line) triclinic system from ref 12; (bold line) orthorhombic system from this work.

Table 3. ^{29}Si NMR Data ($CDCl_3$) for Compounds 2 and 3

compd	δ (ppm)	^2J (Hz)	^3J (Hz)
2a	−0.74	7.24 (6 H)	3.9 (4 H)
2c	−0.02	7.17 (6 H)	unresolved
3a	−1.37	7.0 (6 H)	3.3 (4 H)
3c	−1.24	unresolved	unresolved
2b	−30.20		unresolved
2d	−29.81		unresolved
3b	−30.75		unresolved
3d	−30.57		unresolved

An X-ray crystallographic analysis was also performed for the pyridinophane **2b** and the cyclophane **3a** (Table 2). In contrast to the *syn* geometry of **2a**, the ORTEP drawings show that **2b** and **3a** both adopt a centrosymmetric *anti* conformation in the solid state (Figure 1). Selected distances and angles are given in Table 4. It shows that Si−O and Si−C bond lengths as well as C−Si−C angles are practically the same for both **2b** and **3a** and that they fall in the normal range. Superimposition of the two structures led to RMS = 0.318 Å (only the C_{ipso} atoms were taken into account for the phenyl groups of **2b**). A packing analysis of the crystal lattices reveals no intermolecular π stacking, whatever the compound. We have recently shown[14a] that the disulfite pyridinophane **1** crystallizes in a *syn* conformation very similar to that found for **2a**, whereas the corresponding cyclophane leads to an *anti* one.[14c] From all these results, we concluded that the favored solid-state conformation would be the *anti* one in the case of [5.5]cyclophanes and *syn* in the case of [5.5]-pyridinophanes, unless bulky groups such as $Si(Ph_2)$ are introduced in the bridge. The N···N electrostatic interaction could play an important role in determining the conformation in the solid state.

Table 4. Selected Angles (deg) and Bond Lengths (Å) for Compounds 2a,b and 3a

	Compound **2a**		
C(6)−N(1)−C(2)	119.1(6)	N(1)−C(6)	1.354(9)
N(1)−C(2)−C(26)	112.9(7)	N(1)−C(2)	1.369(9)
N(1)−C(6)−C(7)	115.8(8)	C(6)−C(7)	1.478(11)
O(8)−C(7)−C(6)	113.0(6)	C(7)−O(8)	1.453(11)
C(7)−O(8)−Si(9)	126.9(6)	O(8)−Si(9)	1.624(6)
O(8)−Si(9)−O(12)	111.4(3)	Si(9)−O(12)	1.651(5)
C(11)−Si(9)−C(10)	113.0(7)	Si(9)−C(11)	1.825(12)
C(13)−O(12)−Si(9)	121.3(5)	Si(9)−C(10)	1.839(12)
O(12)−C(13)−C(14)	111.9(7)	O(12)−C(13)	1.421(9)
N(15)−C(14)−C(13)	114.0(7)	C(13)−C(14)	1.498(10)
	Compound **2b**		
O(2)−Si(1)−C(12)	108.9(1)	Si(1)−O(2)	1.633(2)
O(2)−Si(1)−C(18)	104.7(1)	Si(1)−C(12)	1.857(3)
C(12)−Si(1)−C(18)	113.5(1)	Si(1)−C(18)	1.853(3)
Si(1)−O(2)−C(3)	121.9(2)	O(2)−C(3)	1.427(3)
O(2)−C(3)−C(4)	109.5(2)	C(3)−C(4)	1.501(4)
C(3)−C(4)−C(5)	122.1(2)	C(4)−N(9)	1.337(3)
C(3)−C(4)−N(9)	115.4(2)	C(8)−N(9)	1.341(3)
C(7)−C(8)−C(10)	122.3(2)	C(8)−C(10)	1.500(4)
N(9)−C(8)−C(10)	115.3(2)	C(10)−O(11)	1.436(3)
C(4)−N(9)−C(8)	118.2(2)		
C(8)−C(10)−O(11)	110.9(2)		
	Compound **3a**		
C(6)−C(1)−C(7)	119.7(3)	C(1)−C(6)	1.386(4)
C(1)−C(6)−C(5)	120.8(3)	C(1)−C(7)	1.527(4)
C(1)−C(7)−O(8)	110.4(2)	C(5)−C(6)	1.399(4)
C(7)−O(8)−Si(9)	124.9(2)	C(7)−O(8)	1.427(4)
O(8)−Si(9)−C(10)	112.3(1)	O(8)−Si(9)	1.638(2)
O(8)−Si(9)−C(11)	103.9(1)	Si(9)−C(10)	1.853(4)
O(8)−Si(9)−O(12)	111.0(1)	Si(9)−C(11)	1.858(3)
C(10)−Si(9)−C(11)	113.4(2)	Si(9)−O(12)	1.642(2)
C(10)−Si(9)−O(12)	105.1(1)	O(12)−C(13)	1.435(4)
C(11)−Si(9)−O(12)	111.4(1)		
Si(9)−O(12)−C(13)	121.5(2)		

In addition, we wanted to determine the conformational preference of these cyclophanes without the influence of the packing energy. Indeed, the solid-state conformation often is not the true global energy minimum. Examination of literature data shows that the reliance on just the crystal structures is not, in most cases, an infallible and reliable indicator of the conformation in solution or under vacuum.[15] The ^{1}H NMR spectra at room temperature systematically show a sharp singlet for the four CH_2 groups. This chemical shift equivalence of all the methylene protons need not be taken as evidence of a facile *syn*−*anti* interconversion by aromatic ring flipping but could result as well from the free motion of the bridge.[4b,16] The available confor-

(14) (a) Grignon-Dubois, M.; Laguerre, M.; Fayet, J.-P.; Léger, J.-M. *J. Mol. Struct.* **1997**, *415*, 101. (b) The superimposition of the two X-ray structures led to RMS = 0.144 Å for the 12 atoms of the pyridine rings and RMS = 0.550 Å between the silicon and sulfur atoms. (c) Grignon-Dubois, M.; Laguerre, M.; Léger, J.-M. Results to be submitted for publication.

(15) See for example: (a) Wolff, J. J. *Angew. Chem., Int. Ed. Engl.* **1996**, *35*, 2195. (b) Lii, J.-H.; Allinger, N. L. *J. Am. Chem. Soc.* **1989**, *111*, 8576.

(16) Anker, W.; Bushnell, G. W.; Mitchell, R. H. *Can. J. Chem.* **1979**, *57*, 3080.

Table 5. Energy Level (kJ mol^{-1}) and Conformational Features of the Cluster Leaders for Compounds 2 and 3

compd	cluster no.[a]	leader	E^b	Si···Si[c]	N···N or C_1···C_1[c]	C_4···C_4[c]	conformn
2a (115)	1 (75)	1	−117.2	7.7	4.3	3.9	A
	2 (21)	30	−107.1	6.6	4.6	6.8	G
	3 (7)	39	−102.8	6.9	4.2	6.5	G
	4 (4)	84	−103.2	6.5	4.2	6.4	G
	5 (4)	88	−103.1	7.9	3.9	6.9	D
	6 (4)	103	−102.6	8.0	4.1	7.1	D
	XR (no. 1)[d]		**−107.2**	**8.0**	**4.0**	**3.9**	
	XR (no. 1)[e]		**−114.0**	**8.3**	**3.9**	**4.1**	
2a (185)	1 (105)	1	−76.8	6.5	4.5	3.7	A
	2 (41)	23	−71.0	6.6	4.3	7.4	G
	3 (3)	38	−69.3	6.5	3.9	9.0	E
	4 (6)	44	−68.8	6.8	4.3	7.1	G
	5 (9)	45	−68.2	6.5	3.9	9.0	E
	6 (9)	64	−65.5	6.5	4.2	6.5	G
	7 (4)	86	−64.8	6.7	4.4	4.7	B
	8 (2)	122	−64.2	6.6	4.2	3.7	A
	9 (2)	127	−64.1	6.8	4.4	4.8	B
	10 (3)	134	−63.9	6.2	4.9	7.2	C
	11 (1)	144	−63.5	6.9	4.2	6.4	G
	XR[d]		**−34.0**	**7.6**	**4.4**	**8.9**	
3a (474)	1 (106)	1	−10.4	6.4	4.0	3.9	A
	2 (125)	13	−9.5	6.2	4.4	7.6	C
	3 (197)	38	−8.4	5.8	4.4	6.8	G
	4 (16)	220	0.3	6.6	4.0	7.2	F
	5 (8)	279	1.5	7.1	4.6	4.5	B
	6 (12)	305	2.7	7.3	3.9	8.4	E
	7 (9)	374	3.4	7.5	3.9	6.4	G
	8 (1)	471	4.6	6.9	4.0	8.1	F
	XR[d]		**7.5**	**8.2**	**4.1**	**8.5**	
3b (640)	1 (94)	1	28.5	6.6	4.0	3.9	A
	2 (96)	3	28.5	6.5	4.4	4.0	A
	3 (83)	6	28.6	6.7	4.0	8.9	E
	4 (297)	14	29.5	6.7	4.2	6.6	G
	5 (11)	90	32.9	6.6	3.8	7.4	F
	6 (14)	103	33.4	6.6	3.8	7.4	F
	7 (12)	219	36.0	6.7	4.8	7.3	C
	8 (4)	248	36.5	6.5	3.9	7.7	F
	9 (6)	259	36.9	6.5	3.9	7.8	F
	10 (3)	386	39.1	6.6	3.9	9.2	E
	11 (9)	452	40.3	7.1	4.4	5.0	B
	12 (6)	461	40.5	7.0	4.2	5.6	B
	13 (5)	497	41.1	7.0	4.0.4	5.0	B

[a] Number of conformers. [b] In kJ mol^{-1}. [c] Distances in Å. [d] After minimization of the X-ray structure. [e] After minimization of the X-ray structure from ref 12.

mational space of the four cyclic dimers was therefore analyzed by molecular mechanics calculations. To generate all the plausible conformers, we chose to use a Monte Carlo style conformational search (MC) as implemented in MacroModel.[17,18] Indeed, in contrast with dynamics,[19] MC calculations do not provide dynamic information on the system, since particles of the system are simply moved randomly according to statistical rules. Concerning the choice of the force field, MM2* was selected because it led to very good parameters for all molecules, in contrast to MM3*, which led to 76−120 "bad" or "general" parameters, mainly due to the O−Si−O and pyridine moieties.[20] The number of conformers found using an energetic window of 15 kJ mol^{-1} is reported in Table 5.[21] These values show the greater mobility of the metacyclophanes compared to the pyridinophanes and the influence of the silicon atom substituents on this mobility. It is worth noting that the steric energies of pyridinophanes are 105 kJ mol^{-1} (dimethylsilylene) and 107 kJ mol^{-1} (diphenylsilylene) lower than for the corresponding cyclophanes. Examination of the energy components shows that this difference results essentially from the electrostatic term due to the nitrogen atoms. Moreover, the conformational space is considerably restricted by the presence of the nitrogen.

To better understand how the conformations obtained are geometrically related to one another, a cluster analysis was carried out following the MC search. These calculations were performed using the XCluster 1.1 program[22] implemented in Macromodel. The similarity between conformers was evaluated using a distance criterion selection as the RMS difference between all corresponding heavy atoms in pairs of structures (see

(17) Chang, G.; Guida, W. C.; Still, W. C. *J. Am. Chem. Soc.* **1989**, *111*, 4379.

(18) Saunders, M.; Houk, K. N.; Wu, Y. D.; Still, W. C.; Lipton, M.; Chang, G.; Guida, W. C. *J. Am. Chem. Soc.* **1990**, *112*, 1419.

(19) Experience shows that, even at 900 K, a time scale of 500 ps may prove to be sometimes insufficient to allow significant conformational interconversion and sampling.

(20) The MM3 force field has been recently improved by Allinger for silanes, but containing only C−Si or Si−Si linkages: Chen, K.; Allinger, N. L. *J. Phys. Org. Chem.* **1997**, *10*, 697.

(21) With the diphenylsilylated compounds, the free rotations of the phenyl groups about the Si−C bonds were not taken into account.

(22) Shenkin, P. S.; McDonald, D. Q. *J. Comput. Chem.* **1994**, *15*, 899.

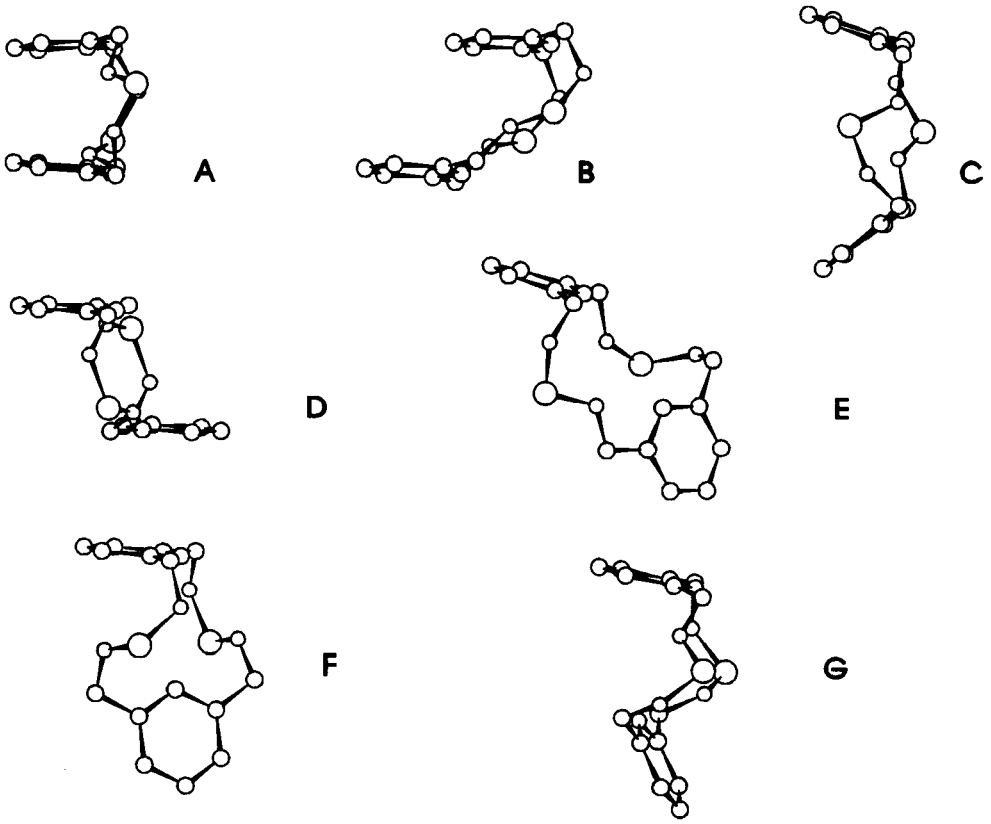

Figure 3. Side views of the calculated typical conformers showing the relationship of the two aromatic rings in the cyclic dimers. See Table 6 for percentage distribution of conformers A−G.

Experimental Section). This approach leads to a set of clusters, each of them being a family of conformers.[23] It is worth noting that the conformers constituting a cluster can be very different in energy but are always close in their overall geometry. The lowest-energy one is defined as the leader of the cluster. The representative leaders of the whole families are listed by ascending energy in Table 5. As predicted, examination of these results shows that the number of conformers is greater for the diphenylsilylene derivatives (**2b**, **3b**) than for the dimethylsilylene ones (**2a**, **3a**). More interesting is the greater difference in energy between the first and the second clusters with pyridinophanes (respectively 10.1 and 5.73 kJ mol^{-1}) than with cyclophanes (0.96 and 0.08 kJ mol^{-1}), which confirms the relative rigidity of the former. The most significant structural characteristics of the cluster leaders and of the solid-state conformations are listed in Table 5. Examination of these values leads to the following comments.

(1) The conformation of the bridge seems to be governed more by the size of the substituents attached to the silicon atoms than by the nature of the aromatic ring. Indeed, the variation of the Si···Si distances is smaller with the diphenylsilylene compounds (respectively 0.7 and 0.6 Å for **2b** and **3b**) than with the dimethylsilylene ones (respectively 1.5 and 1.3 Å for **2a** and **3a**).

(2) The same tendencies are observed for the distances between the two aromatic rings, as shown by the smaller variations of the N···N or C_1 ...C_1 distances for dimethylsilylene derivatives (respectively 0.7 and 0.5 Å for **2a** and **3a**) than for the diphenylsilylene ones (1 Å for both **2b** and **3b**); the same is observed for the variation of the C_4...C_4 distances, but in a larger range. However, these latter values do not give a clear understanding of the ring-flipping process.

Table 6. Distribution (%) of Conformers A−G[a]

	A	B	C	D	E	F	G
2a	65	0	0	7	0	0	28
2b	58	3	2	0	6	0	31
3a	22	2	26	0	3	4	43
3b	30	3	2	0	13	6	46

[a] See Figure 3.

To classify all these families of conformers and allow a comparison of their geometry, a second clusterization was effected based only on the arrangement of the two aromatic rings. It led to seven types of structures, summarized as A−G in Figure 3 and Table 6 with their respective weights. They are representative of four geometries: *syn* or *syn*-like (A−C), *anti* or twisted-*anti* (D, E), orthogonal (F), and anticlinal (G). Table 5 shows that the lowest energy conformer for each compound adopts a *syn* geometry. With the two pyridinophanes **2a** and **2b,** the *syn* geometry is found in the first cluster, which is the most populated (respectively 65 and 58%), the second one being anticlinal (G) in both cases. In contrast, with the cyclophanes **3a**,**b** the most populated clusters are not the first, but the third and the fourth respectively, which also both present an anticlinal arrangement (G). The *anti* arrangement D is never found in the energetic window of 15 kJ mol^{-1} except for

(23) A conformer belongs to a cluster if it lies within the threshold distance of any component of this cluster and at more than this threshold distance of all components of all other clusters.

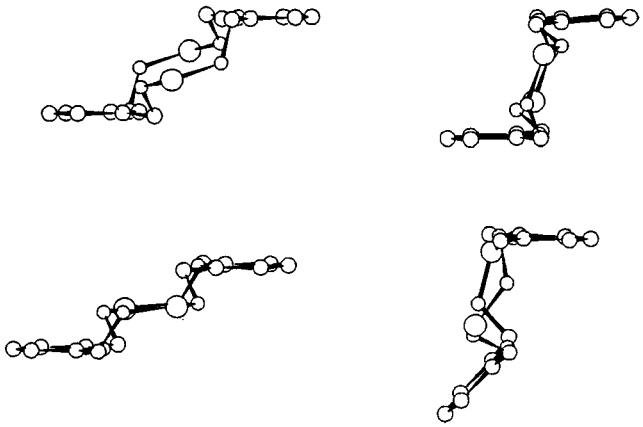

Figure 4. Conformation of the X-ray structure before and after minimization for **2b** and **3a**.

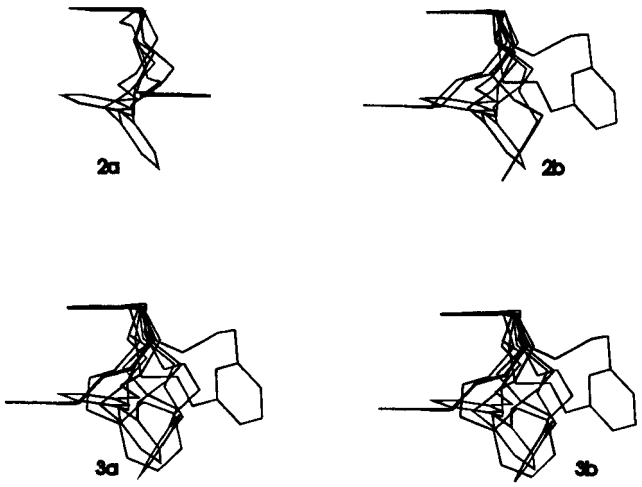

Figure 5. Available conformational space of **2a**,**b** and **3a**,**b**.

the two last clusters of **2a**. The twisted-*anti* structure E is found with **2b**, **3a**, and **3b**, but with a low weight (respectively 6, 3, and 13%). The two *syn* arrangements observed in the solid state for **2a** are found in cluster 1 (75 conformers). In this case, the leader is very close to the X-ray structure obtained by Holmes *et al.*,[12] which in turn is well-represented by the fifth conformer (ΔE = 3.2 kJ mol^{-1}), whereas our X-ray structure for **2a** is represented by the 27th conformer (ΔE = 10.0 kJ mol^{-1}). In contrast, the *anti* solid conformations observed for **3a** and **2b** are respectively 17.5 and 42.8 kJ mol^{-1} higher in energy compared to their respective lowest energy conformer. After minimization, the solid-state conformation of **2b** led to the most stable anticlinal conformation G, while the solid-state conformation of **3a** was globally preserved, with some slight deviations (Figure 4). Starting from the *anti* X-ray structure of **2b** and **3a**, we built the *anti* conformation for **2a** and **3b**. It appears that, with full minimization, these conformations are unstable and immediately revert to an anticlinal conformation. However, using the steepest descent method, which ensures only a local minimization, the *anti* conformation can be optimized and, in the case of **3b**, fully minimized without reversion to the anticlinal form. Under these conditions, the following results were obtained: **2a**, *anti*, ΔE = 23.6 kJ mol^{-1}; **3b**, *anti*, ΔE = 26.35 kJ mol^{-1} (leading to a final energy of −93.6 kJ mol^{-1} for **2a** and 64.9 kJ mol^{-1} for **3b**). These values show that this geometry cannot play a significant role in the conformational equilibrium at room temperature.

The populations of each structure (Figure 3) show that the relative position of the aromatic rings is more dependent on their nature (benzene or pyridine) than on the size of the substituents bound to the silicon. The only exception is the conformation C, which really participates in the ring flipping only with **3a**. The influence of the silicon substituents does not seem to play a significant role in the relative position of the aromatic rings under vacuum. Only a small effect appears in the *anti* conformation, which is found for **2a**, whereas the diphenylsilylene derivatives led to the *anti*-twisted form. The available conformational space for the four derivatives is summarized in Figure 5. In addition, we also performed MM3* calculations under the same conditions as with MM2*. The three products studied by X-ray crystallography, i.e. **2a**,**b** and **3a**, were examined and gave in each case exactly the same *syn* geometry as the lowest energy conformers (RMS ≈ 0.11).

Experimental Section

Melting points were determined on a Metler capillary apparatus and are uncorrected. The ^{1}H and ^{13}C NMR spectra were recorded on a Bruker AC 250 spectrometer, and the ^{29}Si NMR spectra on a Bruker AC 200 fitted with an Aspect 3000 data system using a 10 mm broad-band probe. ^{29}Si chemical shifts were determined using INEPT decoupled experiment.[13a] ^{29}Si proton-coupled spectra were obtained using SPT experiments as previously described[13b] and ^{29}Si proton-selective-decoupled spectra using the refocused INEPT technique.[13c] All the chemical shifts are given in ppm. The ^{29}Si chemical shifts are relative to hexamethyltrisilazane in the case of dimethylsilylene compounds and silicone oil in the case of the diphenylsilylene species. The chemical shifts of these two references were measured relative to TMS under the same experimental conditions (respectively −4.37 and −21.95 ppm). Mass spectra were measured on an AEI MS 12 spectrometer using both FAB and electronic impact techniques. Elemental analyses were performed by the Service Central d'Analyses du CNRS (F-69390 Vernaison, France). Ultrasound-promoted reactions were carried out in a common ultrasonic laboratory cleaner (Brandsonic 321) filled with thermostated water at 20−25 °C. The reaction flask was partially submerged in the sonicator water bath in a place that produced maximum agitation.

Materials. Synthesis grade benzene, 2,6-pyridinedimethanol, and 2,6-benzenedimethanol were purchased from Aldrich and used as received. Chlorosilanes were distilled from magnesium powder prior to use. All reactions were carried out under an argon atmosphere.

Typical Procedure for Cyclization. To a vigorously stirred solution of 2,6-pyridine- or benzenedimethanol (respectively 1.39 or 1.38 g, 10.0 mmol) and triethylamine (2.02 g, 20.0 mmol) in benzene (50 mL) at room temperature was added dropwise within 10 min a solution of freshly distilled chlorosilane (10.0 mmol) in benzene (20 mL). After the addition, the mixture was heated at reflux for 18 h or sonicated at 20−25 °C for 3 h, before the solvent was completely removed in vacuo. The crude product was taken up with dry diethyl ether (100 mL), leading to precipitation of triethylamine hydrochloride, which was removed by filtration. The ethereal solution was evaporated to dryness; then the minimum of diethyl ether (about 20 mL) was added to the residue in order to produce

precipitation of the cyclic dimer. It was isolated by filtration as colorless crystals, while evaporation of the solution led to a viscous oil identified as the oligomers (**2c**,**d**, **3c**,**d**). The cyclic dimer was recrystallized from methylene chloride to give **2a**,**b** or **3a** as white crystals. In the case of **3b**, the solid was quickly washed with water to remove the remaining triethylamine hydrochloride and then recrystallized from chloroform. Yields are reported in Table 1.

1,3,11,13-Tetraoxo-2,12-(dimethylsilylene)[5.5](2,6)-pyridinophane (2a): mp 167−168 °C (CH_2Cl_2); ^{1}H NMR ($CDCl_3$) δ 0.22 (12 H, s), 4.55 (8 H, s), 6.95 (4 H, d, J = 7.70 Hz), 7.33 (2 H, t, J = 7.70 Hz); ^{13}C NMR ($CDCl_3$) δ −3.11, 65.46, 118.54, 136.91, 158.94; ^{29}Si ($CDCl_3$) δ −0.74 (^2J = 7.15 Hz (6 H), ^3J = 4.0 Hz (4 H)); MS, *m*/*z* (%) 390 (M^+, 96.8), 375 (17), 270 (11.8), 254 (38.1), 196 (M/2 + 1, 100), 180 (67.1). Anal. Calcd for $C_{18}H_{26}N_2O_4Si_2$: C, 55.36; H, 6.71; N, 7.17. Found: C, 55.28; H, 6.97; N, 7.24.

Oligomers (2c): colorless oil; ^{1}H NMR ($CDCl_3$) δ 0.17 (6 H, s), 4.77 (4 H, s), 7.22 (2 H, d, J = 7.73 Hz), 7.57 (1 H, t, J = 7.73 Hz); ^{13}C NMR ($CDCl_3$) δ −3.01, 65.54, 118.55, 137.43, 159.53; ^{29}Si ($CDCl_3$) δ −0.02.

1,3,11,13-Tetraoxo-2,12-(diphenylsilylene)[5.5](2,6)-pyridinophane (2b): mp 206 °C (CH_2Cl_2); ^{1}H NMR ($CDCl_3$) δ 4.69 (8 H, s), 7.08 (d, 4 H, J = 7.7 Hz), 7.3−7.47 (14 H, m), 7. 71 (8 H, m); ^{13}C NMR ($CDCl_3$) δ 66.17, 118.92, 128.11, 130.65, 132.41, 134.97, 137.18, 159.13; ^{29}Si ($CDCl_3$) δ −30.16; MS, *m*/*z* (%) 638 (M^+, 20.7), 375 (17), 561 (35.9), 440 (8.8), 242 (100). Anal. Calcd for $C_{38}H_{34}N_2O_4Si_2$: C, 71.45; H, 5.36; N, 4.38. Found: C, 71.61; H, 5.52; N, 4.50.

Oligomers (2d): colorless oil; ^{1}H NMR ($CDCl_3$) δ 4.87 (4 H, s), 7.22−7.36 (11 H, m), 7.62−7.75 (2 H, m); ^{13}C NMR ($CDCl_3$) δ 65.99, 118.70, 128.12, 130.77, 131.72, 135.02, 137.50, 159.98; ^{29}Si ($CDCl_3$) δ −29.81.

1,3,11,13-Tetraoxo-2,12-(dimethylsilylene)[5.5]-metacyclophane (3a): mp 157 °C (CH_2Cl_2); ^{1}H NMR ($CDCl_3$) δ 0.20 (12 H, s), 4.59 (8 H, s), 7.14−7.22 (8 H, m); ^{13}C NMR ($CDCl_3$) δ −2.93, 64.70, 125.85, 125.94, 128.20, 140.55; ^{29}Si ($CDCl_3$) δ −0.90 (^2J = 7.0 Hz (6 H), ^3J = 3.3 Hz (4 H)); MS, *m*/*z* (%) 388 (M^+, 100), 283 (12.5), 270 (13.3), 269 (49.3), 149 (63.1), 121 (65.5), 119 (93.9), 105 (84.8), 104 (85.2). Anal. Calcd for $C_{20}H_{28}O_4Si_2$: C, 61.82; H, 7.26. Found: C, 61.69; H, 7.16.

Oligomers (3c): colorless oil; ^{1}H NMR ($CDCl_3$) δ 0.16 (6 H, s), 4.72 (4 H, s), 7.18−7.32 (4 H, m); ^{29}Si ($CDCl_3$) δ −1.24.

1,3,11,13-Tetraoxo-2,12-(diphenylsilylene)[5.5]-metacyclophane (3b): mp 219 °C ($CHCl_3$); ^{1}H NMR ($CDCl_3$) δ 4.60 (8 H, s), 7.05 (2 H, s), 7.20 (6H, m), 7.35−7.55 (12 H, m), 7.71 (8 H, dd, J = 1.5 Hz, 7.7 Hz); ^{13}C NMR ($CDCl_3$) δ 65.23, 125.44, 125.85, 127.93, 127.99, 128.19, 130.44, 132.56, 134.97, 140.25; ^{29}Si ($CDCl_3$) δ −30.75; MS, *m*/*z* (%) 636 (M^+, 66.3), 558 (8.2), 561 (35.9), 437 (10.3), 361 (18.6), 259 (27.9), 224 (20.8), 199 (100), 181 (97.5). Anal. Calcd for $C_{40}H_{36}O_4Si_2$: C, 75.43; H, 5.70. Found: C, 75.31; H, 5.68.

Oligomers (3d): colorless oil; ^{1}H NMR ($CDCl_3$) δ 4.71 (4 H, s), 7.28−7.52 (10 H, m), 7.75 (4H, dd, J = 1.3 Hz, 7.6 Hz); ^{13}C NMR ($CDCl_3$) δ 64.97, 124.73, 125.47, 128.05, 128.37, 130.57, 132.38, 135.09, 140.39; ^{29}Si ($CDCl_3$) δ −30.57.

X-ray Structural Determination of 2a,b and 3a. The colorless crystals used had approximate dimensions of 0.30 × 0.20 × 0.10 mm for **2a**, 0.17 × 0.42 × 0.42 mm for **2b**, and 0.25 × 0.30 × 0.07 mm for **3a**. Data were collected on an Enraf-Nonius CAD-4 diffractometer using graphite-monochromated CuKα radiation up to a Bragg angle of 65°. Cell constants were determined by least-squares refinement of diffractometer angles for reflections collected in the range 25° < θ < 30°. Crystal and relevant X-ray data for the three compounds are summarized in Table 2. In the case of **2b** and **3a**, the molecules sit on a center of symmetry.

The structures were solved using the MITHRIL program[24] and refined by the block-diagonal least-squares method. An *E* map revealed the oxygen and silicon atoms. The non-hydrogen atoms were located from difference Fourier syntheses. Lorentz and polarization corrections as well as an empirical (ψ scans) absorption correction were applied. The projections of the molecules showing the numbering scheme adopted are shown in Figure 1.

Molecular Mechanics Calculations. Calculations were performed on a SGI Indy 4400 SC platform running Macromodel version 5.0 (Columbia University, New York, NY).[25] Conformational minima were found using the modified MM2* (1987 parameters) force field as implemented and completed in the MacroModel program. The built structures were minimized to a final RMS gradient ≤0.005 kJ Å^{-1} mol^{-1} *via* the truncated Newton Conjugate Gradient (TNCG) method (500 cycles). The starting geometries used in the calculations were the X-ray conformation for both **2a**,**b** and **3a.** For **3b**, we started from the geometry obtained by replacing the two nitrogen atoms in **2b** by CH groups.

Monte Carlo Style Conformational Search. This search is implemented in MacroModel.[17,18] The automatic setup has been selected: i.e. single bonds variable, chiral centers set, and flexible ring opened. To ensure convergence, 3000 steps were made per input structure in an energy range of 15 kJ mol^{-1}. Each conformer was fully minimized (500 cycles, TNCG method, RMS ≤0.005 kJ Å^{-1} mol^{-1} with MM2* force field). The least-used structures were used as starting geometries only if their energies were within the energetic window (15 kJ mol^{-1} of the lowest energy structure yet found). In all cases, the extended cutoff option (EXNB) was used: 12 Å for VdW and 20 Å for electrostatics.

XCluster Analysis. We used the XCluster 1.1 program implemented in MacroModel.[22] For this purpose, we used a distance criterion selection as the RMS difference between all corresponding heavy atoms in pairs of structures. The variation of the clustering level *vs* the separation ratio are depicted in Figures 6−9 (Supporting Information). For each compound, the best accuracy level was chosen from these plots as leading to the highest separation ratio. These calculations led to the following results (Table 5).

2a: 115 conformers, X-cluster (threshold 0.818 Å, level 98) gave 18 families, which number was finally reduced to 6 on account of symmetry (conformer leaders: 1−30−39−84−88−103). The first family (75 conformers) corresponds to a *syn* arrangement of the aromatic rings. The lowest energy conformer is very close to the X-ray structure described by Holmes,[12] which in turn is well represented by the fifth conformer (ΔE = 3.2 kJ mol^{-1}).

2b: 185 conformers, X-cluster (threshold 0.524 Å, level 161) gave 25 families, which number was finally reduced to 11 on account of symmetry (conformer leaders: 1−23−38−44−45−64−86−122−127−134−144). The first family contains 105 conformers with a *syn* arrangement of the aromatic rings. The fifth conformer (ΔE = 1.92 kJ mol^{-1}) is similar to the X-ray structure of the methyl derivative **2a**.[12] The minimized X-ray *anti* structure was found to be 21.1 kJ mol^{-1} higher than the lowest energy conformer.

3a: 474 conformers, X-cluster (threshold 0.727 Å, level 452) gave 23 families, which number was finally reduced to 8 on account of symmetry (conformer leaders: 1−13−38−220−279−305−374−471). The first family (106 conformers) also presents a *syn* arrangement of the aromatic rings, the lowest energy conformer being identical with the X-ray structure of **2a.**[12] The minimized X-ray *anti* structure was found to be 17.9 kJ mol^{-1} higher in energy.

3b: 640 conformers, X-cluster (threshold 0.725 Å, level 618) gave 23 families, which number was finally reduced to 13 on account of symmetry (conformer leaders: 1−3−6−14−90−103−219−248−259−386−452−461−497). The first family (94

(24) Gilmore, C. J. *J. Appl. Crystallogr.* **1984**, *17*, 42.
(25) Mohamadi, F.; Richards, N. G. J.; Guida, W. C.; Liskamp, R.; Lipton, M.; Caufield, C.; Chang, G.; Hendrikson, T.; Still, W. C. *J. Comput. Chem.* **1990**, *11*, 441.

conformers) also presents a *syn* arrangement of the aromatic rings.

Acknowledgment. Part of this work was supported by Rhône-Poulenc SA and the Conseil Régional d'Aquitaine. We thank Dr. S. Mignani for fruitful discussions.

Supporting Information Available: Tables giving positional and thermal parameters and bond distances and angles for **2a**,**b** and **3a** (13 pages). Ordering information is given on any current masthead page.

OM9704758